Macromolecular Rapid Communications
www.mrc-journal.de

Tunable Dual-Thermoresponsive Core–Shell Nanogels Exhibiting UCST and LCST Behavior

*Robin Rajan and Kazuaki Matsumura**

Thermoresponsive polymers change their physical properties as the temperature is changed and have found extensive use in a number of fields, especially in tissue engineering and in the development of drug delivery systems. The synthesis of a novel core–shell nanogel composed of *N*-isopropylacrylamide and sulfobetaine by reversible addition fragmentation chain transfer polymerization is reported. The core–shell architecture of the nanogels is confirmed using energy dispersive X-ray spectroscopy in scanning transmission electron microscopy. These nanogels exhibit dual thermoresponsive behavior, i.e., the core of the nanogel exhibits lower critical solution temperature, while the shell displays upper critical solution temperature behavior. Transition temperatures can be easily tuned by changing the molecular weight of the constituent polymer. These nanogels can be efficiently used in temperature-triggered delivery of therapeutic proteins and drugs.

Stimuli-responsive or smart polymers have attracted considerable interest in several fields, e.g., biomedicine, nanotechnology, and numerous others, due to their versatility.[1,2] Such systems exhibit an attractive feature, i.e., stimuli-responsiveness, owing to their increased functionality which makes them suitable for applications in several fields.[3,4] Among several known stimuli, temperature and pH are most commonly investigated for biomaterial applications. However, typically, these systems require two types of stimuli, which increases the complexity, thereby limiting their extensive use. Hence, a system requiring a single stimulus, rather than multiple stimuli, i.e., a single stimulus for a dual response, can increase its overall applicability.[5] Recently, much research has been carried out to develop systems that show dual thermoresponsive behavior, such as lower critical solution temperature (LCST)–LCST and upper critical solution temperature (UCST)–LCST types of block copolymers.[6] A previous study by Yin et al. demonstrated the formation of schizophrenic core–shell microgels via seeded emulsion polymerization which showed both LCST and UCST transitions.[7] Several more studies have been carried out successfully using dual thermoresponsive systems for different biomedical applications;[8–10] however, this behavior has been investigated mostly with polymeric systems such as non-crosslinked linear block copolymers. In a recent study, Yoshimitsu et al. prepared a shape switching dual responsive di-block copolymer using polymerized ionic liquid and 2-methoxyethyl vinyl ether.[11] Nevertheless, a significantly more efficient system can be created using nanogels instead. This is because nanogels offer numerous advantages as compared to simple polymeric systems, e.g., greater control over drug release, higher biocompatibility, sustainability, and good permeability.[12] In addition, because nanogels are small in size, their surface areas are large, permitting facile molecule encapsulation.[13] Owing to these properties, nanogels have been widely used as delivery agents for drugs, proteins, and genes.[12,14] Thus, the incorporation of the dual-responsive behavior with nanogels[15] can augment their advantages, resulting in the creation of a novel and more efficient system.

Several polymers, e.g., poly(*N*,*N*-diethylacrylamide)[16–20] and polyampholytes,[21,22] exhibiting LCST behavior have been reported. Among these polymers, poly(*N*-isopropylacrylamide) (poly(NIPAM)) is one of the most extensively investigated polymer for its LCST behavior.[23,24] Poly(NIPAM) systems have been used for various applications, e.g., gene delivery[25] and regulation of cell attachment and detachment.[26] On the contrary, not many polymers exhibiting UCST transitions have been reported. In an earlier study, a random copolymer of methacrylic acid and 2-(dimethylamino)ethyl methacrylate exhibiting UCST in ethanol–water and methanol–water solvent mixtures was reported.[27] The use of solvent mixtures, including organic solvent, for thermal transitions limits its application for biomedical uses. An and his coworkers recently synthesized polymeric systems which exhibit UCST.[28,29] Polysulfobetaine (poly-SPB) has been widely reported to exhibit UCST behavior in water.[30,31] Apart from the thermoresponsive behavior, poly-SPB has been previously used for applications such as anti-bioadherent coatings,[32] cryopreservation,[33,34] and protein aggregation inhibition,[35,36] and many other biomedical applications.[37,38]

Reversible addition fragmentation chain transfer (RAFT) polymerization is one of the most widely used polymerization techniques and is a versatile method for bestowing living features to radical polymerization. It is applicable to a wide range of monomers and can tolerate various reaction conditions and

Dr. R. Rajan, Prof. K. Matsumura
School of Materials Science
Japan Advanced Institute of Science and Technology
1-1 Asahidai, Nomi, Ishikawa 923-1292, Japan
E-mail: mkazuaki@jaist.ac.jp

The ORCID identification number(s) for the author(s) of this article can be found under https://doi.org/10.1002/marc.201700478.

DOI: 10.1002/marc.201700478

solvents.[39] Moreover, RAFT polymerization does not involve the use of any metal catalyst, making it ideal for biomaterial applications. The RAFT agent can be easily cleaved from the end product (deprotection of the end group) by reduction with $NaBH_4$,[40] thus eliminating any unnecessary effect of the RAFT agent. RAFT polymerization facilitates the preparation of nanogels with great control of the structures and properties. In a previous study, thermoresponsive microgels consisting of P(MEO_2MA-*co*-OEGMA) were prepared by free radical emulsion polymerization with surfactants as stabilizers.[41] Surfactants are generally considered toxic and require multiple purification steps to be removed from the final system.[42,43] The need to use surfactants for the preparation of nanogels can be eliminated by preparing hydrophilic macrochain transfer agents (macro-CTAs) by RAFT polymerization.[44] Recently, Sanson and Rieger reviewed conventional and controlled radical polymerization techniques and processes in preparing nano-/microgels.[45]

With this in mind, core–shell nanogels were synthesized from NIPAM and SPB, where the thermoresponsive property of each component was exploited, affording a system exhibiting UCST and LCST behavior. A particularly interesting application of these systems could be in the delivery of therapeutic proteins, because of the potency of poly-SPB based systems to suppress protein aggregation,[35] which is currently hampering further development of protein-based biological formulations.[46]

The nanogels were synthesized in two steps. First, SPB was polymerized into its corresponding homopolymer (**Scheme 1**a). The kinetic study of RAFT-mediated polymerization was conducted by ^{1}H NMR spectroscopy (Figure S1, Supporting Information) and the reaction completion was monitored by observing the loss of vinyl protons from the monomer. Conversion of the monomer to the corresponding polymers, and the relationship between $\ln([M]_o/[M])$ and time was also monitored by ^{1}H NMR (Figure S2, Supporting Information); a linear curve was obtained, indicating that polymerization follows first-order reaction kinetics, representative of a living polymerization.[47] ^{1}H and ^{13}C NMR spectroscopy (Figures S3 and S4, Supporting Information) of the final product (polymer) after purification was obtained to characterize the polymers. Gel permeation chromatography (GPC) curves indicated that all of the polymers had a unimodal distribution (Figure S5, Supporting Information), with polydispersity index (M_w/M_n) well within the range of living polymerization, and observed M_n values consistent with the theoretical molecular weight for the corresponding feed ratios.

RAFT polymerization afforded a homopolymer with a functional end group, serving as a macro-CTA (new RAFT agent) for the subsequent reaction. Consequently, NIPAM was polymerized in the presence of the previously synthesized macro-CTA and a chemical crosslinker (ethylene glycol dimethacrylate), thus forming a core–shell nanogel, with crosslinked poly-(NIPAM) and poly-SPB as the core and shell, respectively (Scheme 1b).

Two nanogels with different degrees of polymerization for poly-SPB were prepared. Dynamic light scattering (DLS) and transmission electron microscopy (TEM) were employed to characterize these nanogels. DLS measurements (Figure S6, Supporting Information) confirmed the formation of nanogels. A summary of the characteristics of the polymers is provided in **Table 1**.

TEM measurements clearly showed the formation of spherical nanogels and the formation of a core–shell architecture (**Figure 1**a and Figure S7, Supporting Information), represented by a relatively darker core than the shell. Since the shell is made up of poly-SPB, which is sulfur-rich, and the core is sulfur-deficient, nanogels were characterized by a scanning TEM (STEM) equipped with a high-angle annular dark-field (HAADF) detector and energy dispersive X-ray spectroscopy (EDX). Results unambiguously demonstrated the formation of a core–shell structure. STEM–HAADF image shows the presence of two distinct regions in the nanogel (Figure 1b), indicating the

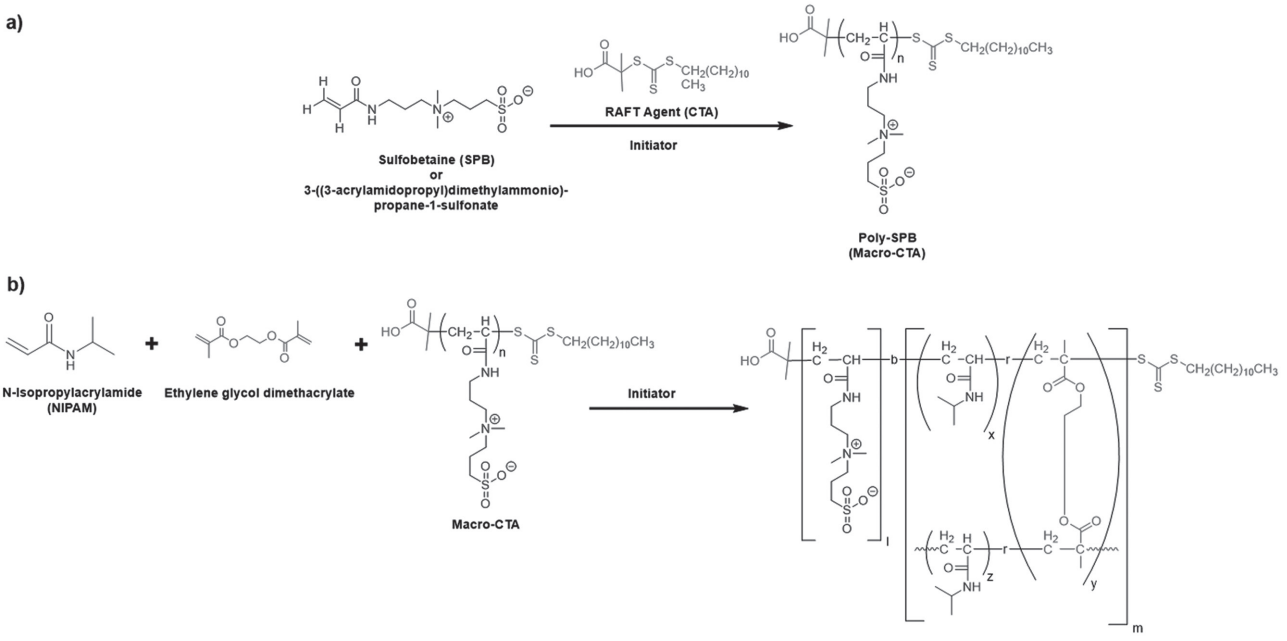

Scheme 1. Synthesis of a) poly-SPB and b) core–shell nanogel by RAFT polymerization.

Table 1. Characteristics of macro-CTA and nanogels via RAFT polymerization.

Nanogel	Shell (macro-CTA)	Macro-CTA			Core	Molar ratio[a)]	Hydrodynamic diameter [nm][b)]
		Molar ratio[c)]	$M_n \times 10^{-3}$,[d)]	M_w/M_n[d)]			
NG-1	Poly-$(SPB)_{200}$	1000:1:5	36.2	1.59	NIPAM	1000:1.67:5:20	532.5 ± 0.2 (0.19)[e)]
NG-2	Poly-$(SPB)_{100}$	500:1:5	21.1	1.37	NIPAM	500:1.67:5:20	483.8 ± 0.2 (0.17)[e)]

[a)][NIPAM]:[Initiator]:[Macro-CTA]:[crosslinker] used for the synthesis of nanogels; [b)]Determined by DLS; [c)][Monomer]:[Initiator]:[RAFT agent] used for the synthesis of macro-CTA; [d)]Determined by GPC; [e)]Polydispersity index, determined by DLS.

presence of a distinct core and a shell. Figure 1c shows EDX elemental mapping images of NG-2. The red color represents carbon (C), dark blue represents nitrogen (N), turquoise blue represents oxygen (O), and green represents sulfur (S). Sulfur is present only in the shell of the nanogel (indicated by green color), while no sulfur was seen in the core, thus supporting the formation of a core–shell nanogel consisting of a poly-SPB shell (sulfur-rich) and cross-linked NIPAM core (sulfur-deficient). To confirm this further, STEM-EDX line analysis was done (Figure 1d); it was clearly seen that carbon, nitrogen, and oxygen are distributed all over the nanogel (carbon's intensity is more pronounced in the core due to the crosslinking), while sulfur is present only near the shell, indicated by the appearance of green bands only in the region which corresponds to the shell of the nanogel. To our knowledge, this is the first study to conclusively show the formation of a polymeric core–shell architecture.

To ascertain the thermoresponsiveness of these nanogels, photographs of the nanogel solution at different temperatures were taken (**Figure 2**a). Heating or cooling this solution resulted in coacervate formation. On resting/centrifuging this solution during cooling/heating, liquid-phase separation occurred (for clarity, the solution is stained with alizarin red). This experiment clearly demonstrated that these nanogels exhibit LCST and UCST behavior.

From Figure 1c, it was clearly seen that the size of the core greatly exceeds the size of the shell; hence, the soluble shell should be able to only partially prevent the aggregation (partial shielding) of the core when the temperature is raised. This was confirmed by the observation that while the nanogels showed

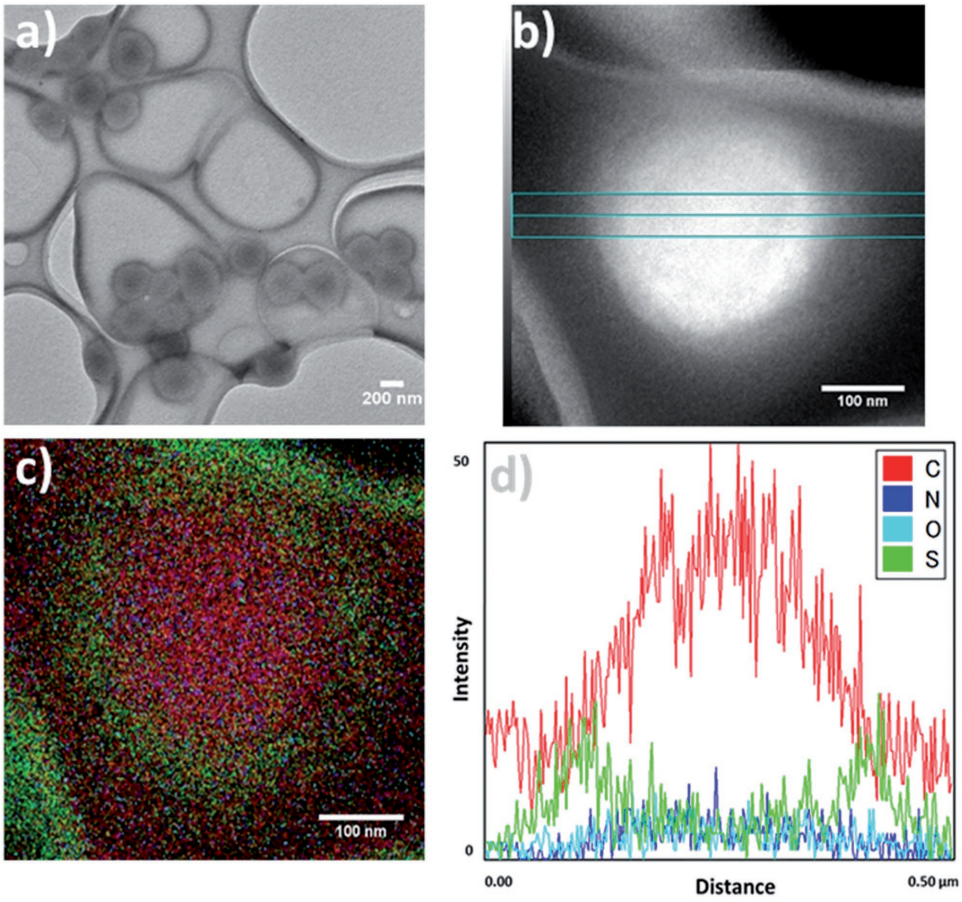

Figure 1. a) TEM image, b) STEM-HAADF, c) EDX elemental mapping image, and d) STEM-EDX line analysis of NG-2.

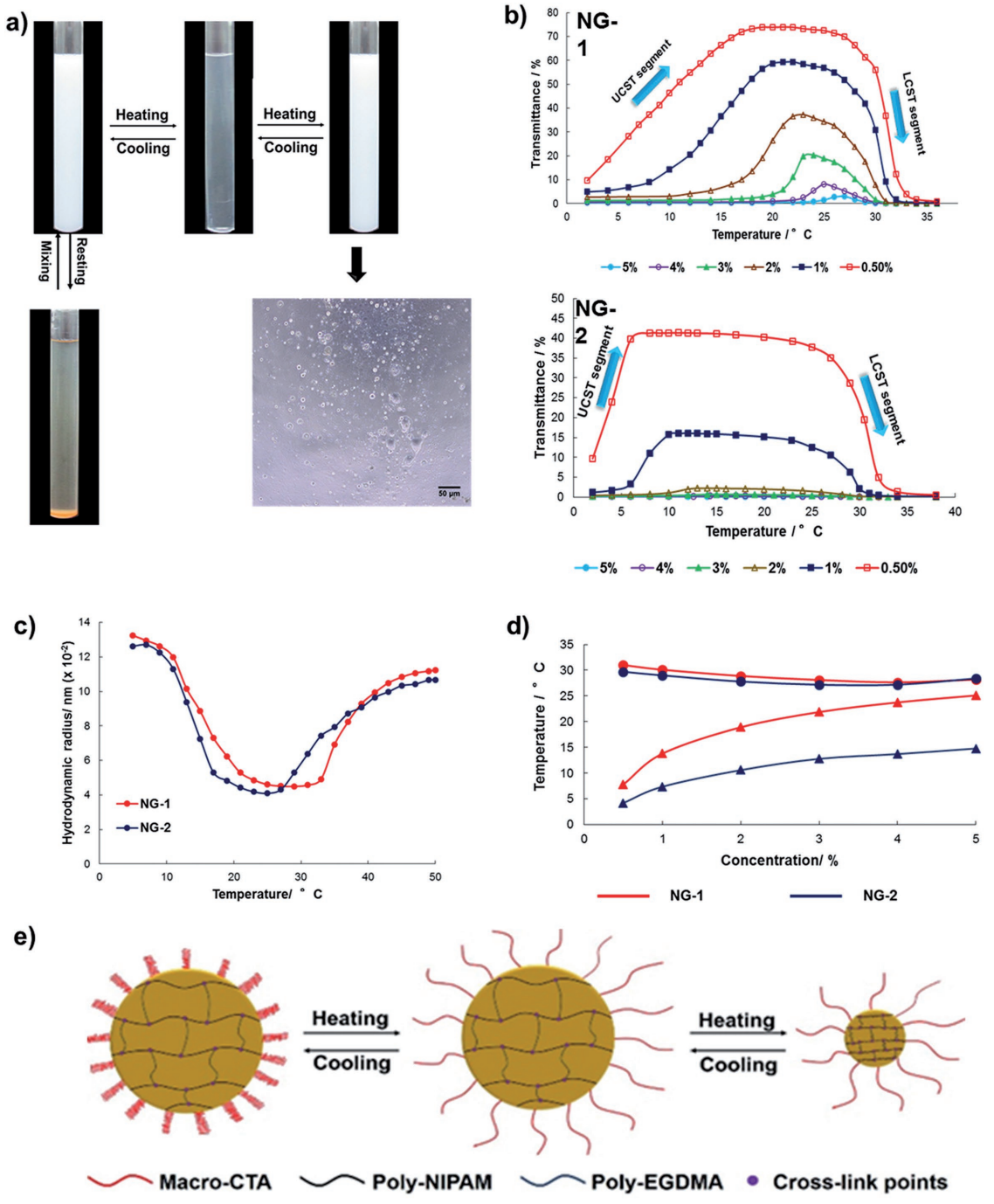

Figure 2. Thermoresponsive behavior of aqueous solution of nanogels. a) Photographs of the nanogel (NG-1, 1% polymer concentration) before and after cooling. The photograph at the left was taken at 4 °C, the middle at 25 °C, and on the right at 37 °C. The solution on the bottom-left was stained with alizarin red (10 μg mL^{-1}) to enhance the visibility; microphotograph shows that nanogels form coacervate droplets on phase separation; b) transmittance of aqueous solutions of NG-1 and NG-2 at various concentrations; c) variable-temperature DLS measurements (heating process) of nanogels in water at a concentration of 0.5%; d) phase diagram of the aqueous solution of NG-1 and NG-2, circles represent LCST transition and triangles represent UCST transitions; e) schematic representation of the LCST and UCST transitions of nanogels on cooling and heating.

a clear UCST transition leading to liquid–liquid phase separation, LCST transition was not as clearly observed. By lowering the temperature, phase separation took place immediately upon resting (without the need for centrifugation), whereas when the temperature was raised, only an increase in turbidity was observed. Two different phases were not observed on resting (phase separation took place only after centrifugation at a high speed).

Next, to quantitatively evaluate the thermoresponsive property of the as-formed nanogels, their transmittance values at

various temperatures were measured by UV–vis spectroscopy at 550 nm. Figure 2b shows the phase-separation behavior of an aqueous solution of NG-1 and NG-2 at various concentrations. Initially, on increasing the temperature, an increase in transmittance was observed and, after reaching a maximum value, transmittance became constant for a certain temperature interval, thus depicting UCST behavior. Upon further increasing the temperature, transmittance started decreasing and, after 30 °C, transmittance values dropped down to below 5%. An increase in temperature beyond 30 °C led to transmittance being stable, indicating LCST behavior of the NIPAM core. With decreasing and increasing temperatures, the nanogels exhibited UCST and LCST behavior, respectively. The phase-separation temperatures for both LCST and UCST behavior changed with the nanogel concentration. The UCST transition of nanogels was compared with macro-CTA and it was found that transition temperature (cloud point) of macro-CTA corresponds well with that of the nanogel (Figure S8, Supporting Information). The thermal transitions of the nanogels were further investigated using DLS (Figure 2c). Results unambiguously demonstrated that both the nanogels show two thermal transitions upon heating from 5 to 50 °C and the transition temperatures were close to the values determined by turbidity measurements.

From the corresponding plots of phase-separation behavior, phase diagrams for the two nanogels were plotted and cloud points, which represent the point at which the transmittance reaches half of its maximum value, were determined.[22] From Figure 2d, it was seen that phase-separation temperature (cloud points) of the nanogels was highly dependent on the polymer concentration. Moreover, with the change in the degree of polymerization of poly-SPB (maintaining the NIPAM concentration constant), only the UCST phase-separation temperatures changed because, with increasing molecular weight, the entropy of mixing decreased, resulting in increased UCST.[48] Changing the poly-SPB concentration (which constitutes the nanogel shell) did not significantly affect the properties of the poly-(NIPAM) unit, indicating that the core and shell of the nanogel exhibit independent behavior with respect to their thermoresponsive behavior. This result indicated that the phase-transition temperatures could be easily tuned via the change in the molecular weights of the constituent polymers.

Next, we investigated the effect of common salt (NaCl) on phase separation. When nanogel was dissolved in NaCl solution, the hydrodynamic radius decreased, which could be due to the dissociation of interchain association.[49] Moreover, the addition of the aqueous NaCl solutions altered the phase transition temperature of the nanogels (Figure S9, Supporting Information). A noticeable change was observed even at very low NaCl concentrations. This is supported by previous reports, which suggested that the ionic strength of the NaCl markedly affects polyampholyte conformation as well as the intra- and intermolecular electrostatic interactions.[50,51]

The core–shell nanogels consisted of poly-SPB and poly-(NIPAM) crosslinked with poly(ethylene glycol dimethacrylate) as the shell and core, respectively. With decreasing temperature, poly-SPB in the shell exhibited shrinkage, whereas the nanogel core remained intact. On the other hand, on heating, the poly-(NIPAM)-rich core exhibited shrinkage (Figure 2e).

In conclusion, core–shell nanogels showing dual thermoresponsive behavior, i.e., exhibiting both UCST and LCST transitions, were synthesized. To the best of our knowledge, this is the first report of the development of a nanogel system which conclusively establishes the core–shell architecture. The cloud points for the transition temperature can be easily tuned via the change in the molecular weights of the constituent polymers. Our results suggested that this approach can afford nanogels, which can be extremely useful in various fields, e.g., drug delivery and biosensing, as well as for the development of thermoresponsive scaffolds. Studies to further optimize these nanogel systems with respect to tuning of the UCST and LCST according to the target application via the modification of polymer parameters and introduction of small amounts of an additional monomer are currently underway.

Supporting Information

Supporting Information is available from the Wiley Online Library or from the author.

Acknowledgements

The authors thank Mr. Koichi Higashimine, Japan Advanced Institute of Science and Technology, for assistance in STEM measurement and analysis.

Conflict of Interest

The authors declare no conflict of interest.

Keywords

nanogels, phase-separation, polymers, TEM, thermoresponsive

Received: July 13, 2017
Revised: August 18, 2017
Published online:

[1] M. A. C. Stuart, W. T. S. Huck, J. Genzer, M. Muller, C. Ober, M. Stamm, G. B. Sukhorukov, I. Szleifer, V. V Tsukruk, M. Urban, F. Winnik, S. Zauscher, I. Luzinov, S. Minko, *Nat. Mater.* **2010**, *9*, 101.
[2] M. Wei, Y. Gao, X. Li, M. J. Serpe, *Polym. Chem.* **2017**, *8*, 127.
[3] L. Zhang, R. Guo, M. Yang, X. Jiang, B. Liu, *Adv. Mater.* **2007**, *19*, 2988.
[4] D. Schmaljohann, *Adv. Drug Delivery Rev.* **2006**, *58*, 1655.
[5] S. Liu, S. P. Armes, *Angew. Chem., Int. Ed.* **2002**, *41*, 1413.
[6] Y. Kotsuchibashi, M. Ebara, T. Aoyagi, R. Narain, *Polymers* **2016**, *8*, 380.
[7] J. Yin, J. Hu, G. Zhang, S. Liu, *Langmuir* **2014**, *30*, 2551.
[8] F. Dai, P. Wang, Y. Wang, L. Tang, J. Yang, W. Liu, H. Li, G. Wang, *Polymer* **2008**, *49*, 5322.
[9] Y. Chang, W.-Y. Chen, W. Yandi, Y.-J. Shih, W.-L. Chu, Y.-L. Liu, C.-W. Chu, R.-C. Ruaan, A. Higuchi, *Biomacromolecules* **2009**, *10*, 2092.
[10] Z. Dong, J. Mao, D. Wang, M. Yang, W. Wang, S. Bo, X. Ji, *Macromol. Chem. Phys.* **2014**, *215*, 111.

[11] H. Yoshimitsu, E. Korchagina, A. Kanazawa, S. Kanaoka, F. M. Winnik, S. Aoshima, *Polym. Chem.* **2016**, *7*, 2062.
[12] N. Singh, V. Gill, P. Gill, *Am. J. Adv. Drug Delivery* **2013**, *1*, 271.
[13] R. T. Chacko, J. Ventura, J. Zhuang, S. Thayumanavan, *Adv. Drug Delivery Rev.* **2012**, *64*, 836.
[14] T. Nochi, Y. Yuki, H. Takahashi, S. Sawada, M. Mejima, T. Kohda, N. Harada, I. G. Kong, A. Sato, N. Kataoka, D. Tokuhara, S. Kurokawa, Y. Takahashi, H. Tsukada, S. Kozaki, K. Akiyoshi, H. Kiyono, *Nat. Mater.* **2010**, *9*, 572.
[15] Y. Li, Z. Ye, L. Shen, Y. Xu, A. Zhu, P. Wu, Z. An, *Macromolecules* **2016**, *49*, 3038.
[16] E. S. Gil, S. M. Hudson, *Prog. Polym. Sci.* **2004**, *29*, 1173.
[17] M. A. Cole, N. H. Voelcker, H. Thissen, H. J. Griesser, *Biomaterials* **2009**, *30*, 1827.
[18] A. Valentin, L. Cardamone, S. Baek, J. D. Humphrey, *J. R. Soc., Interface* **2009**, *6*, 293.
[19] V. Aseyev, H. Tenhu, F. M. Winnik, in *Self Organized Nanostructures of Amphiphilic Block Copolymers II* (Eds: A. H. E. Müller, O. Borisov), Springer, Berlin, **2011**, pp. 29–89.
[20] A. Halperin, M. Kröger, F. M. Winnik, *Angew. Chem., Int. Ed.* **2015**, *54*, 15342.
[21] A. Abdilla, S. Shi, N. A. D. Burke, H. D. H. Stöver, *J. Polym. Sci., Part A: Polym. Chem.* **2016**, *54*, 2109.
[22] E. Das, K. Matsumura, *J. Polym. Sci., Part A: Polym. Chem.* **2016**, *55*, 1.
[23] H. G. Schild, *Prog. Polym. Sci.* **1992**, *17*, 163.
[24] T. Okano, N. Yamada, M. Okuhara, H. Sakai, Y. Sakurai, *Biomaterials* **1995**, *16*, 297.
[25] M. D. Lavigne, S. S. Pennadam, J. Ellis, L. L. Yates, C. Alexander, D. C. Górecki, *J. Gene Med.* **2007**, *9*, 44.
[26] D. Cunliffe, C. de las Heras Alarcón, V. Peters, J. R. Smith, C. Alexander, *Langmuir* **2003**, *19*, 2888.
[27] Q. Zhang, R. Hoogenboom, *Chem. Commun.* **2015**, *51*, 70.
[28] W. Sun, Z. An, P. Wu, *Macromolecules* **2017**, *50*, 2175.
[29] X. Cao, Z. An, *Macromol. Rapid Commun.* **2015**, *36*, 2107.
[30] J. Ning, K. Kubota, G. Li, K. Haraguchi, *React. Funct. Polym.* **2013**, *73*, 969.
[31] P. A. Woodfield, Y. Zhu, Y. Pei, P. J. Roth, *Macromolecules* **2014**, *47*, 750.
[32] A. B. Lowe, M. Vamvakaki, M. A. Wassall, L. Wong, N. C. Billingham, S. P. Armes, A. W. Lloyd, *J. Biomed. Mater. Res.* **2000**, *52*, 88.
[33] R. Rajan, F. Hayashi, T. Nagashima, K. Matsumura, *Biomacromolecules* **2016**, *17*, 1882.
[34] R. Rajan, M. Jain, K. Matsumura, *J. Biomater. Sci., Polym. Ed.* **2013**, *24*, 37.
[35] R. Rajan, K. Matsumura, *J. Mater. Chem. B* **2015**, *3*, 5683.
[36] R. Rajan, K. Matsumura, *Sci. Rep.* **2017**, *7*, 45777.
[37] S. Kudaibergenov, W. Jaeger, A. Laschewsky, *Supramolecular Polymers/Polymeric Betains/Oligomers*, Springer, Berlin **2006**, pp. 157–224.
[38] S. Jiang, Z. Cao, *Adv. Mater.* **2010**, *22*, 920.
[39] Y. Mitsukami, M. S. Donovan, A. B. Lowe, C. L. McCormick, *Macromolecules* **2001**, *34*, 2248.
[40] H. Kitano, T. Kondo, T. Kamada, S. Iwanaga, M. Nakamura, K. Ohno, *Colloids Surf., B* **2011**, *88*, 455.
[41] T. Cai, M. Marquez, Z. Hu, *Langmuir* **2007**, *23*, 8663.
[42] J.-H. Ryu, R. T. Chacko, S. Jiwpanich, S. Bickerton, R. P. Babu, S. Thayumanavan, *J. Am. Chem. Soc.* **2010**, *132*, 17227.
[43] Y. Kotsuchibashi, R. Narain, *Polym. Chem.* **2014**, *5*, 3061.
[44] Z. An, Q. Qiu, G. Liu, *Chem. Commun.* **2011**, *47*, 12424.
[45] N. Sanson, J. Rieger, *Polym. Chem.* **2010**, *1*, 965.
[46] W. Wang, *Int. J. Pharm.* **2005**, *289*, 1.
[47] J. Chiefari, Y. K. (Bill) Chong, F. Ercole, J. Krstina, J. Jeffery, T. P. T. Le, R. T. A. Mayadunne, G. F. Meijs, C. L. Moad, G. Moad, E. Rizzardo, S. H. Thang, *Macromolecules* **1998**, *31*, 5559.
[48] J. Seuring, S. Agarwal, *Macromol. Rapid Commun.* **2012**, *33*, 1898.
[49] S. E. Kudaibergenov, *Polyampholytes: Synthesis, Characterization and Application*, Springer, Boston, MA **2002**, pp. 137–152.
[50] S. Nath, C. S. Patrickios, T. A. Hatton, *Biotechnol. Prog.* **1995**, *11*, 99.
[51] A. B. Lowe, C. L. McCormick, *Chem. Rev.* **2002**, *102*, 4177.

